



WARSAW UNIVERSITY OF TECHNOLOGY
FACULTY OF ELECTRONICS
AND INFORMATION TECHNOLOGY
INSTITUTE OF RADIOELECTRONICS

Report No. 12, 2004

**A Survey of Properties of Ambiguity Functions
of Analytic, Quaternionic and Monogenic Signals**

by Grzegorz Hahn

Warsaw, 1 December 2004

Institute of Radioelectronics, Nowowiejska 15/19, 00-665 Warsaw, tel./fax: (4822) 8255248

Abstract: The paper investigates the properties of ambiguity functions of 2-D analytic, quaternionic and monogenic signals. In the introduction the notions of the above signals and their Wigner distributions and ambiguity functions are recalled. The properties of the ambiguity functions are investigated using two kinds of test signals: A band-pass test signal in the form of a sum of two harmonic signals with a Gaussian envelope and a low-pass signal in the form of the analytic, quaternionic and monogenic signals with a real part of a Gaussian signal of the same form as the Gaussian 2-D probability density function of correlated random variables.

Keywords –4-D Wigner distributions and ambiguity functions, 2-D analytic, quaternionic and monogenic signals

1. Introduction.

The concept of the ambiguity function (AF) has been defined in 1953 by Woodward [1] in considerations about the target resolution of radars. The AF of the complex time signal $\psi(t)$ is given by the inverse Fourier transform of the correlation product $r(t, \tau) = \psi(t + \tau/2) \cdot \psi(t - \tau/2)$, i.e.,

$$AF(\mu, \tau) = \int r(t, \tau) e^{-j2\pi\mu t} dt$$

where μ is the frequency shift variable (frequency lag or Doppler),

and τ the time shift variable (time lag or delay). Much earlier (1932) Wigner defined a multidimensional distribution called nowadays the Wigner distribution [2]. Its 2-D version is a time-frequency distribution defined by the Fourier transform of $r(t, \tau)$, i.e., $W(t, f) = \int r(t, \tau) e^{-j2\pi f \tau} d\tau$.

The $AF(\mu, \tau)$ and $W(t, f)$ are forming a pair of 2-D Fourier transforms, $W(t, f) \stackrel{2FT}{\Leftrightarrow} AF(\mu, \tau)$.

Differently to Wigner, Woodward defined only the 2-D version of the AF . We consider 4-D AF 's, a direct extension of the notion of the Woodward's AF . Consider a 2-D signal $u(x_1, x_2)$, which may represent a 2-D black-white image. In this paper we deal with analytic signals $\psi(x_1, x_2)$ [3], [4], corresponding to $u(x_1, x_2)$, and also with quaternionic [5], [6], and monogenic signals [7], [8], corresponding to $u(x_1, x_2)$. The properties of the 4-D AF 's of these signals are investigated.

2. Preliminaries.

The 2-D Fourier transform of the real signal $u(x_1, x_2)$ is:

$$U(f_1, f_2) = \iint u(x_1, x_2) e^{-j2\pi(f_1 x_1 + f_2 x_2)} dx_1 dx_2, \quad (1)$$

where the spectrum $U(f_1, f_2)$ has a four quadrant support. However, due to the Hermitian symmetry, the signal $u(x_1, x_2)$ may be recovered by the knowledge of the spectrum in a half plane, for example, the half plane $f_1 > 0$. This half plane is a union of two quadrants, the first with $(f_1 > 0, f_2 > 0)$ and the third with $(f_1 > 0, f_2 < 0)$. The single quadrant spectra are:

$$\Gamma_{1,2}(f_1, f_2) = [1 + \text{sgn}(f_1)][1 \pm \text{sgn}(f_2)]U(f_1, f_2), \quad (2)$$

where the plus sign stands for Γ_1 with a support in the first quadrant, and the minus sign for the Γ_2 with the support in the third quadrant. The inverse Fourier transform of Γ_1 yields the analytic signal [3], [4],

$$\psi_1(x_1, x_2) = u(x_1, x_2) - v(x_1, x_2) + j[v_1(x_1, x_2) + v_2(x_1, x_2)] \quad (3)$$

and of Γ_2 the analytic signal

$$\psi_2(x_1, x_2) = u(x_1, x_2) + v(x_1, x_2) + j[v_1(x_1, x_2) - v_2(x_1, x_2)], \quad (4)$$

where

$$v(x_1, x_2) = u(x_1, x_2) ** \frac{1}{\pi^2 x_1 x_2} \quad (5)$$

is the total Hilbert transform of $u(x_1, x_2)$ and $v_1(x_1, x_2) = u(x_1, x_2) ** \frac{\delta(x_2)}{\pi x_1}$ and

$v_2(x_1, x_2) = u(x_1, x_2) ** \frac{\delta(x_1)}{\pi x_2}$ are partial Hilbert transforms [3],[4]. The energies of the

signals ψ_1 and ψ_2 differ except the case of separable signals, i.e., $u(x_1, x_2) = u_1(x_1)u_2(x_2)$.

The recently defined quaternionic [5], [6] and monogenic signals [7], [8] are based on the notion of the Quaternionic Fourier Transform (*QFT*). The *QFT* of a real signal $u(x_1, x_2)$ has the form:

$$QFT(f_1, f_2) = \iint e^{-i2\pi f_1 x_2} u(x_1, x_2) e^{-j2\pi f_2 x_2} dx_1 dx_2$$

$$= A(f_1, f_2) + iB(x_1, x_2) + jC(x_1, x_2) + kD(x_1, x_2), \quad (6)$$

where i, j, k are imaginary units each equal $\sqrt{-1}$. The algebra of quaternions is non-commutative and obeys the rules $ij = -ji = k$, $ki = -ik = j$, $jk = -kj = i$. Due to the noncommutativity the order of functions in the integral (6) cannot be changed. However, the QFT is invertible, and the inverse QFT^{-1} has the form

$$QFT^{-1}[QFT(f_1, f_2)] = u(x_1, x_2) = \iint e^{i2\pi f_1 x} QFT(f_1, f_2) e^{j2\pi f_2 x_2} df_1 df_2. \quad (7)$$

The QFT obeys the rules of a quaternionic Hermitian symmetry, which differs from the Hermitian symmetry of the 2-D FT [6]. In consequence, the signal $u(x_1, x_2)$ can be recovered by a single quadrant part of the QFT . The QFT may be calculated using the 2-D Fourier spectrum $U(f_1, f_2)$ [9]:

$$QFT(f_1, f_2) = \frac{(1-k)}{2} U(f_1, f_2) + \frac{(1+k)}{2} U(-f_1, f_2). \quad (8)$$

Notice, that if $U(f_1, f_2) = U(-f_1, f_2)$, then the $QFT=FT$.

3. The quaternionic signal with a single quadrant spectrum

The quaternionic single-quadrant spectrum is defined by the equation [5], [6]

$$\Gamma_q(f_1, f_2) = [1 + \text{sgn}(f_1)][1 + \text{sgn}(f_2)]QFT(f_1, f_2). \quad (9)$$

The inverse QFT of this spectrum

$$QFT^{-1}[\Gamma_q(f_1, f_2)] = \iint e^{i2\pi f_1 x_1} \Gamma_q(f_1, f_2) e^{j2\pi f_2 x_2} df_1 df_2 \quad (10)$$

yields the following quaternionic signal

$$\psi_q(x_1, x_2) = u(x_1, x_2) + iv_1(x_1, x_2) + jv_2(x_1, x_2) + kv(x_1, x_2), \quad (11)$$

where v_1, v_2 and v are the same Hilbert transforms as applied in the analytic signals (3) and

(4). The conjugate quaternionic signal is

$$\psi_q^*(x_1, x_2) = u(x_1, x_2) - iv_1(x_1, x_2) - jv_2(x_1, x_2) - kv(x_1, x_2). \quad (12)$$

4. The monogenic signal

The monogenic signal is a quaternion-valued function of the form [7], [8],

$$\psi_M(x_1, x_2) = u(x_1, x_2) + iv_{r_1}(x_1, x_2) + jv_{r_2}(x_1, x_2), \quad (13)$$

$$\psi_M^*(x_1, x_2) = u(x_1, x_2) - iv_{r_1}(x_1, x_2) - jv_{r_2}(x_1, x_2) \quad (14)$$

with

$$v_{r_1}(x_1, x_2) = u(x_1, x_2) ** \frac{x_1}{2\pi(\sqrt{x_1^2 + x_2^2})^3} = u(x_1, x_2) ** r_1(x_1, x_2), \quad (15)$$

$$v_{r_2}(x_1, x_2) = u(x_1, x_2) ** \frac{x_2}{2\pi(\sqrt{x_1^2 + x_2^2})^3} = u(x_1, x_2) ** r_2(x_1, x_2). \quad (16)$$

The functions $v_{r_1}(x_1, x_2)$ and $v_{r_2}(x_1, x_2)$ are called Riesz transforms of u . The *QFT* of the Riesz kernels r_1 and r_2 are

$$r_1(x_1, x_2) = \frac{x_1}{2\pi(\sqrt{x_1^2 + x_2^2})^3} \stackrel{QFT}{\Leftrightarrow} \frac{-if_1}{\sqrt{f_1^2 + f_2^2}}, \quad (17)$$

$$r_2(x_1, x_2) = \frac{x_2}{2\pi(\sqrt{x_1^2 + x_2^2})^3} \stackrel{QFT}{\Leftrightarrow} \frac{-jf_2}{\sqrt{f_1^2 + f_2^2}}. \quad (18)$$

Therefore, the frequency domain definition of v_{r_1} and v_{r_2} is

$$v_{r_1}(x_1, x_2) = QFT^{-1} \left[\frac{-if_1}{\sqrt{f_1^2 + f_2^2}} QFT(f_1, f_2) \right], \quad (19)$$

$$v_{r_2}(x_1, x_2) = QFT^{-1} \left[\frac{-jf_2}{\sqrt{f_1^2 + f_2^2}} QFT(f_1, f_2) \right]. \quad (20)$$

The quaternionic spectrum of the monogenic signal is

$$\Gamma_M(f_1, f_2) = QFT[\psi_M(x_1, x_2)] = QFT[u(x_1, x_2)] \left[1 + \frac{f_1 + f_2}{\sqrt{f_1^2 + f_2^2}} \right]. \quad (21)$$

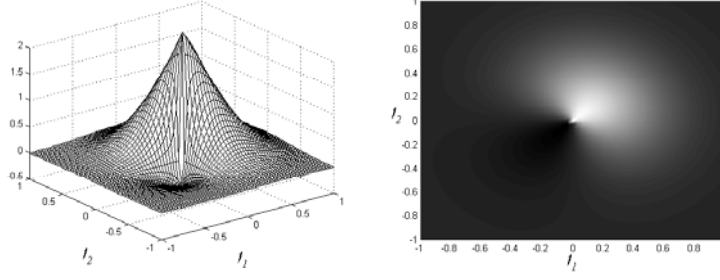


Fig.1. The spectrum of a Gaussian monogenic signal. The main part of the spectrum has a single quadrant support with leakages into the neighbouring quadrants [7]. .

Fig.1 shows Γ_M for the Gaussian signal $u(x_1, x_2) = e^{-\pi(x_1^2 + x_2^2)}$. The Riesz transforms are also called „isotropic” Hilbert transforms.[10].

5. Ambiguity functions

5.1. Ambiguity functions of analytic signals

The ambiguity functions of the 2-D analytic signals $\psi_1(x_1, x_2)$ and $\psi_2(x_1, x_2)$, (See Eq.(3),(4)), are defined as inverse Fourier transforms of the correlation products [11], [12], [13],

$$r_{1,2}(x_1, x_2, \chi_1, \chi_2) = \psi_{1,2}(x_1 + \chi_1/2, x_2 + \chi_2/2) \psi_{1,2}^*(x_1 - \chi_1/2, x_2 - \chi_2/2), \quad (22)$$

where the subscripts 1 or 2 stands for ψ_1 or ψ_2 . The inverse Fourier transform defining the ambiguity function is

$$AF_{1,2}(\mu_1, \mu_2, \chi_1, \chi_2) = \iint r_{1,2}(x_1, x_2, \chi_1, \chi_2) e^{j2\pi(\mu_1 x_1 + \mu_2 x_2)} dx_1 dx_2. \quad (23)$$

The integration is w.r.t. the spatial domain variables (x_1, x_2) in the domain of the frequency shift variables (μ_1, μ_2) . The corresponding Wigner distribution is defined by the Fourier transform of the same correlation product (22)

$$W_{1,2}(x_1, x_2, f_1, f_2) = \iint r_{1,2}(x_1, x_2, \chi_1, \chi_2) e^{-j2\pi(f_1 \chi_1 + f_2 \chi_2)} d\chi_1 d\chi_2. \quad (24)$$

The integration is w.r.t. the spatial shift variables (χ_1, χ_2) in the domain of the frequency variables (f_1, f_2) . For any complex analytic signal the Wigner distribution is always a real function. Differently, the ambiguity function is a complex function, i.e.,

$$AF_{1,2}(\mu_1, \mu_2, \chi_1, \chi_2) = \text{Re}_{1,2}(\mu_1, \mu_2, \chi_1, \chi_2) + j \text{Im}_{1,2}(\mu_1, \mu_2, \chi_1, \chi_2). \quad (25)$$

The insertion in the Eq. (23) the correlation product given by the inverse Fourier transform of (24) yields the following relation between the AF and WD

$$AF_{1,2}(\mu_1, \mu_2, \chi_1, \chi_2) = \iiint W_{1,2}(x_1, x_2, f_1, f_2) e^{j2\pi(\mu_1 x_1 + \mu_2 x_2 + f_1 \chi_1 + f_2 \chi_2)} dx_1 dx_2 df_1 df_2. \quad (26)$$

We have a Fourier pair

$$AF_{1,2}(\mu_1, \mu_2, \chi_1, \chi_2) \stackrel{4F}{\Leftrightarrow} W_{1,2}(\mu_1, \mu_2, f_1, f_2). \quad (27)$$

The $AF_{1,2}$ can be alternatively calculated using the Fourier transform of the frequency domain correlation product

$$g_{1,2}(f_1, f_2, \mu_1, \mu_2) = \Gamma_{1,2}(f_1 + \mu_1/2, f_2 + \mu_2/2) \Gamma_{1,2}^*(f_1 - \mu_1/2, f_2 - \mu_2/2). \quad (28)$$

We get

$$AF_{1,2}(\mu_1, \mu_2, \chi_1, \chi_2) = \iint g_{1,2}(f_1, f_2, \mu_1, \mu_2) e^{-j2\pi(f_1 \chi_1 + f_2 \chi_2)} df_1 df_2. \quad (29)$$

This formula yields exactly the same distribution, as defined by (23). However in many cases the frequency domain algorithm yields large savings in the computation time. Specific forms of AF_1 are derived in Appendix A.

5.2. Ambiguity functions of quaternionic and monogenic signals

The ambiguity functions and Wigner distributions of quaternionic and monogenic signals [14] are defined using the QFT of the following correlation products. The correlation product of the quaternionic signal defined by the Eq.(29) is

$$r_q(x_1, x_2, \chi_1, \chi_2) = \psi_q(x_1 + \chi_1/2, x_2 + \chi_2/2) \psi_q^*(x_1 - \chi_1/2, x_2 - \chi_2/2). \quad (30)$$

The correlation product of the monogenic signal defined by the Eq.(30) has the same form as (22), if only we replace the subscripts „1,2” by „q” or by „M”. The ambiguity function of the quaternionic signal is

$$AF_q(\mu_1, \mu_2, \chi_1, \chi_2) = \iint e^{j2\pi\mu_1x_1} r_q(x_1, x_2, \chi_1, \chi_2) e^{j2\pi\mu_2x_2} dx_1 dx_2. \quad (31)$$

The corresponding Wigner distribution is

$$W_q(x_1, x_2, f_1, f_2) = \iint e^{-i2\pi f_1 x_1} r_q(x_1, x_2, \chi_1, \chi_2) e^{-j2\pi f_2 x_2} d\chi_1 d\chi_2. \quad (32)$$

Let us remind, that the order of functions in the integrals cannot be changed. The equations (31),(32) apply for monogenic signals, if we change the subscripts „q” to „M”. The insertion in (31) the correlation product given by the inverse *QFT* of W_q given by (32) yields

$$AF_q(\mu_1, \mu_2, \chi_1, \chi_2) = \iint e^{j2\pi\mu_1x_1} \left\{ \iint e^{j2\pi f_1 x_1} W_q(x_1, x_2, f_1, f_2) e^{j2\pi f_2 x_2} df_1 df_2 \right\} e^{j2\pi\mu_2x_2} dx_1 dx_2. \quad (33)$$

This relation corresponds to the 4-D Fourier transform given for analytic signals by the Eq.(27). The AF_q and AF_M can not be alternatively calculated using the quaternionic version of (29) (see [14]).

6. Investigations of the properties of ambiguity functions using test signals

6.1. Cross-sections („slices”) of 4-D functions

The ambiguity functions of 2-D signals are 4-D functions. The representation of such functions using 3-D mesh images or 2-D surface images is possible using the notion of a cross section (or „slice”). We present the cross-sections of $AF(\mu_1, \mu_2, \chi_1, \chi_2)$ using fixed values of the spatial shift variables $\chi_1 = \chi_{10}$ and $\chi_2 = \chi_{20}$. We get a 2-D function $AF(\mu_1, \mu_2, \chi_{10}, \chi_{20})$.

In descriptions of images we shall use the notation $AF(\mu_1, \mu_2, 0, 0)$ or $AF(\mu_1, \mu_2, 0.5, 0.5)$,

i.e., $\chi_{10} = 0, \chi_{20} = 0$ or $\chi_{10} = 0.5, \chi_{20} = 0.5$.

6.2. The choice of the test functions

It is well known, that the Wigner distributions and ambiguity functions of a signal having a form of a sum of n individual signals contain auto-terms and cross-terms. Test signals with a large number of auto-terms produce a lot of cross-terms. The comparison of the properties of such distributions is difficult or even impossible. In consequence, we use the test functions

with a single or a double number of auto-terms. We apply two kinds of test functions: Band-pass test functions and low pass test functions . Let us mention, that distributions of real signals instead of analytic, quaternionic and monogenic signal contain much more cross-terms. For example, a real 2-D signal may be written in terms of analytic signals using the formula [4]

$$u(x_1, x_2) = \frac{\psi_1 + \psi_1^* + \psi_2 + \psi_2^*}{4}, \quad (34)$$

where ψ_1 and ψ_2 are the analytic signal defined by the Eqs.(3) and (4) and the Fourier transform of the correlation product

$$r(x_1, x_2, \chi_1, \chi_2) = u\left(x_1 + \frac{\chi_1}{2}, x_2 + \frac{\chi_2}{2}\right) u\left(x_1 - \frac{\chi_1}{2}, x_2 - \frac{\chi_2}{2}\right) \quad (36)$$

which is a sum of 16 terms produces a large number of cross-terms.

6.3. A band-pass test functions

Consider a real signal; of the form :

$$u(x_1, x_2) = e^{-\pi(x_1^2 + x_2^2)} \left[A_1 \cos(2\pi f_{11} x_1) \cos(2\pi f_{12} x_2) + A_2 \cos(2\pi f_{21} x_1) \cos(2\pi f_{22} x_2) \right] \quad (37)$$

The corresponding analytic signal has the form :

$$\psi_{1,2}(x_1, x_2) = e^{-\pi(x_1^2 + x_2^2)} \left[A_1 e^{j2\pi[f_{11}x_1 \mp f_{12}x_2]} + A_2 e^{j2\pi[f_{11}x_1 \pm f_{12}x_2]} \right] \quad (38)$$

where the plus sign stands for ψ_1 and the minus sign for ψ_2 . The Fourier transform (spectrum) of (38) is

$$U_{1,2}(f_1, f_2) = A_1 e^{-\pi(f_1 - f_{11})^2} e^{-\pi(f_2 \pm f_{11})^2} + A_2 e^{-\pi(f_1 - f_{21})^2} e^{-\pi(f_1 \mp f_{22})^2} . \quad (39)$$

. In fact, the signals ψ_1 and ψ_2 are approximately analytic, if the frequencies f_{11}, f_{12}, f_{21} and f_{22} are sufficiently large and the leakage of the spectrum (39) into other quadrants is negligible.

6.4. A low pass test function

We apply a Gaussian low-pass test signal :

$$u(x_1, x_2) = \frac{1}{\sqrt{1-R^2}} \exp \left[-\frac{\pi}{1-R^2} (x_1^2 + x_2^2 - 2Rx_1x_2) \right] \quad (40)$$

This signal has the same form, as the Gaussian probability density function of a sum of two correlated random variables and R is called the correlation coefficient. The spectrum of this signal is

$$U(f_1, f_2) = e^{-\pi(f_1^2 + f_2^2 - 2Rf_1f_2)} \quad (41)$$

The corresponding analytic signals are given by the Eqs. (3) and (4) , the quaternionic signal by the Eq.(11) and the monogenic signal by the Eq.(13).

7. Selected images of cross-sections of ambiguity functions and Wigner distributions

The following images present selected cross-sections of ambiguity functions of test functions of analytic, quaternionic and monogenic signals. Few cross-sections of Wigner distributions are presented to enable comparisons. The images are produced using Matlab graphics with data calculated using C++ code. Since the ambiguity functions are complex or quaternionic valued the corresponding magnitudes (absolute values) are displayed.

7.1. Images for the AF's and WD's of a band-pass signal (see Eq.38)

The cross-sections are presented for fixed values of the spatial coordinates ($\chi_1 = \chi_{10}$, $\chi_2 = \chi_{20}$) and the following values of the modulation frequencies: $f_{11} = f_{12} = 1.5$ and $f_{21} = f_{22} = 3$.

Ambiguity functions of analytic signals $\psi_1(x_1, x_2)$ and $\psi_2(x_1, x_2)$

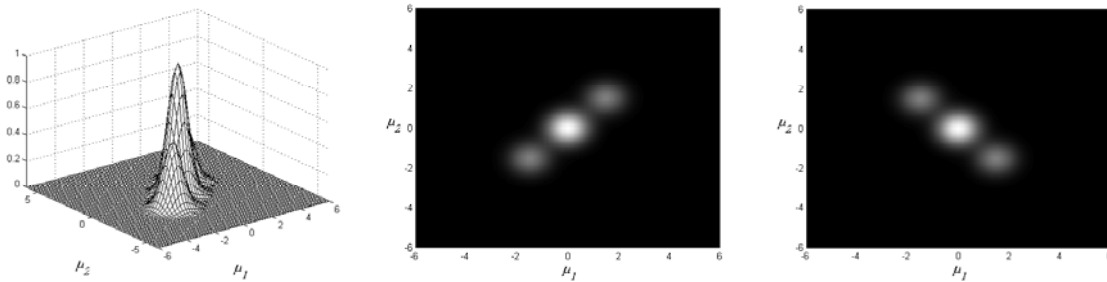


Fig.2. Left, mesh image, center, surface image of $|AF_1(\mu_1, \mu_2, 0, 0)|$, and right, surface image of $|AF_2(\mu_1, \mu_2, 0, 0)|$.

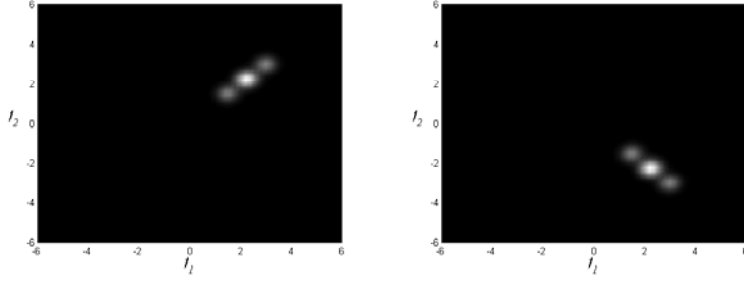


Fig.3. The Cross-section of the Wigner distributions $W_1(f_1, f_2, 0, 0)$ (right) and $W_2(f_1, f_2, 0, 0)$ (left) corresponding to the cross-sections of AF_1 and AF_2 of Fig.1.

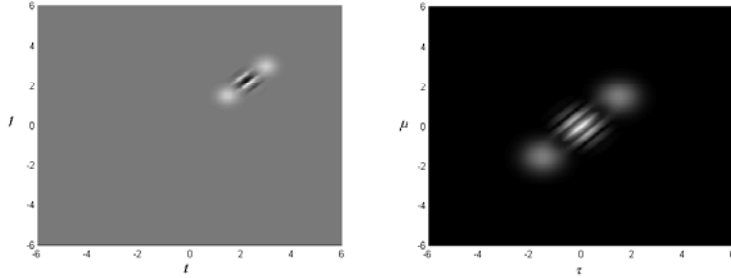


Fig.4. For comparison with Fig.1 and 2 the Wigner distribution $W(t, f)$ (left) and the magnitude of the ambiguity function $|AF(\mu, \tau)|$ (right) are displayed for the of the signal

$$\psi(t) = \exp[-\pi(t-t_1)^2] \exp(j2\pi f_1 t) + \exp[-\pi(t-t_2)^2] \exp(j2\pi f_2 t) \text{ with } t_1 = 1.5, t_2 = 3, f_1 = 1.5, f_2 = 3.$$

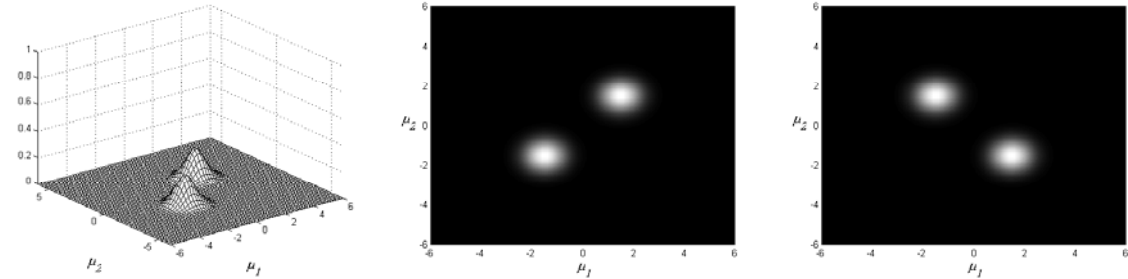


Fig.5 Left, mesh image, center, surface image of $|AF_1(\mu_1, \mu_2, 0.5, 0.5)|$, and right, surface image of $|AF_2(\mu_1, \mu_2, -0.5, 0.5)|$. However, in the not displayed $|AF_2(\mu_1, \mu_2, 0.5, 0.5)|$ the central auto-term is not cancelled.

Let us compare the properties of the cross-sections of the Wigner distributions $W_1(f_1, f_2, 0, 0)$ and $W_2(f_1, f_2, 0, 0)$, displayed in Fig.3 with the corresponding magnitudes of $AF_1(f_1, f_2, 0, 0)$ and $AF_2(f_1, f_2, 0, 0)$ displayed in Fig.2. The Wigner distributions have a single quadrant support, W_1 in the first and W_2 in the third quadrant. Since the band-pass signal defined by the Eq.(38) is a separable function, $W_2(f_1, f_2, 0, 0)$ is represented by the mirror image of $W_1(f_1, f_2, 0, 0)$. We say that W_1 and W_2 contain the same spectral information. The distributions W_1 and W_2 contain two auto-

terms and in between a cross term of a double crest value w.r.t. the auto-terms.. Differently, the auto-terms of $|AF_1(f_1f_2, 0, 0)|$ and of $|AF_2(f_1f_2, 0, 0)|$ located in the origin correspond to a sum of the auto-terms of $W_1(f_1f_2, 0, 0)$ or of $W_2(f_1f_2, 0, 0)$. This summation yields an auto-term of double crest value w.r.t. the two cross-terms. located symmetrically around the origin.. Again, $|AF_1|$ and $|AF_2|$ contain the same spectral information . The only difference is, that cross-terms of $|AF_1|$ and $|AF_2|$ are displayed in different quadrants. There are some similarities of the images of W_1 of Fig.3 and the $|AF_1|$ of Fig. 2 with the Wigner distribution $W(t, f)$ and the magnitude of the ambiguity function $|AF(\mu\tau)|$ of a 1-D time signal $\psi(t) = e^{-\pi(t-t_1)^2} e^{j2\pi f_1 t} + e^{-\pi(t-t_2)^2} e^{j2\pi f_2 t}$. The WD and $|AF|$ of this signal are displayed in Fig.4. The difference between the WD_1 of Fig.3 and the WD of Fig.4 is that the cross-terms of the WD are oscillating functions in comparison to the uni-polar cross-terms of WD_1 .

The image of Fig.5 presents the cross section corresponding to Fig.2, but for the shift variables $\chi_1 = \chi_2 = 0.5$. We observe an interesting phenomenon of cancellation of the auto-terms. Remark: This cancellation occurs for opposite signs of the shift variable χ_1 in $|AF_1(\mu_1, \mu_2, 0.5, 0.5)|$ and $|AF_2(\mu_1, \mu_2, -0.5, 0.5)|$.

Ambiguity functions of quaternionic signals $\psi_q(x_1, x_2)$

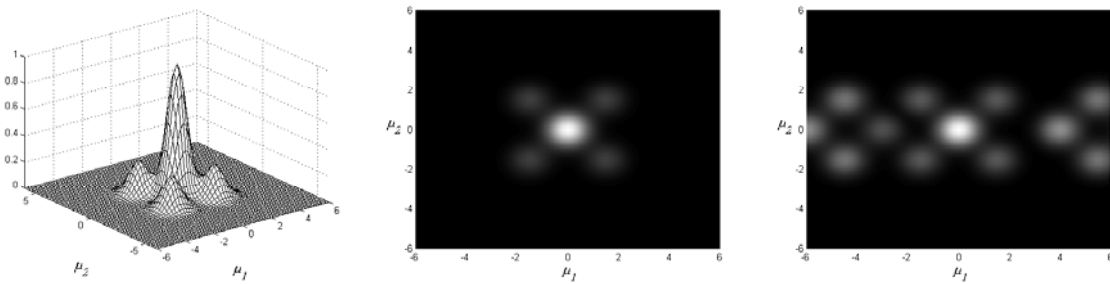


Fig.6. Left, mesh image, center, surface image of $|AF_q(\mu_1, \mu_2, 0, 0)|$, and right, surface image of $AF_q(f_1, f_2, 0.05, 0.05)$.

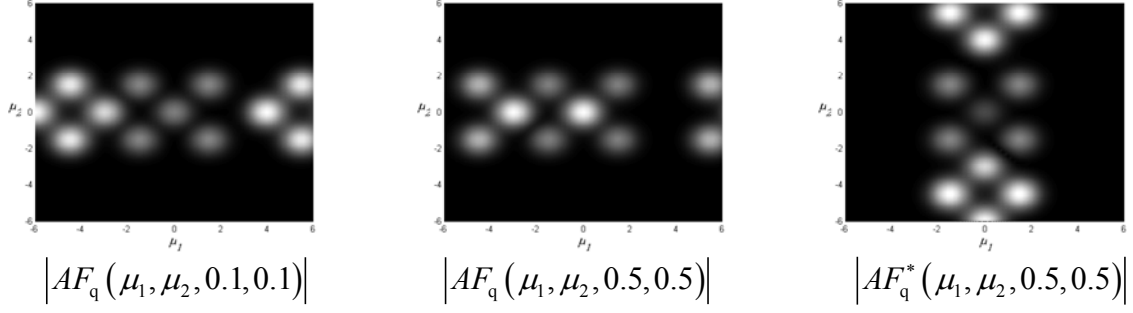


Fig.7. Continuation of Fig.5.

The cross-sections of the magnitude of the ambiguity function of the quaternionic version of the test signal (38) are displayed in Figs.6 and 7. The cross-section $|AF_q(\mu_1, \mu_2, 0, 0)|$, i.e., for zero values of the shift variables $\chi = (\chi_1, \chi_2)$, should be compared with $|AF_1(\mu_1, \mu_2, 0, 0)|$ and $|AF_2(\mu_1, \mu_2, 0, 0)|$ of Fig.2. We observe, that $|AF_q|$ is a sum of $|AF_1|$ and $|AF_2|$. This summation yields the auto-term in the origin of a crest value four times bigger w.r.t, the cross-terms, which are located in all four quadrants and have the same crest value, as the cross-terms of $|AF_1|$ and $|AF_2|$. The above described summation is expected having in mind, that the quaternionic signal $\psi_q(x_1, x_2)$ replaces the two analytic signals $\psi_1(x_1, x_2)$ and $\psi_2(x_1, x_2)$. However, for cross-sections with non-zero values of the shift variables the things are more complicated. Let us compare the cross-sections

$|AF_1(\mu_1, \mu_2, 0.5, 0.5)|$ and $|AF_2(\mu_1, \mu_2, -0.5, 0.5)|$ of Fig.5 with the cross-section

$|AF_q(\mu_1, \mu_2, 0.5, 0.5)|$ of Fig.7. The cancellation of the auto-terms observed in Fig.5 does not exist in

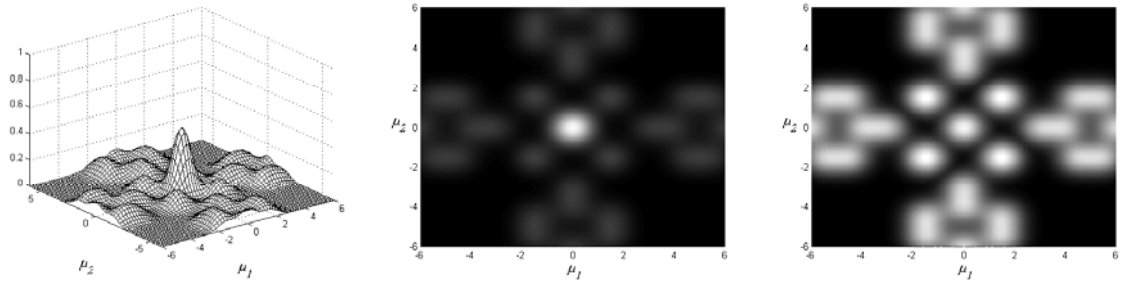
Fig.7, since the cancellation requires different signs of the shift variable χ_1 in $|AF_1|$ and $|AF_2|$. The

images in Fig.7 and 7 show, that a duplicate of the cross-terms is shifted in both direction of the horizontal line. However, for the conjugate correlation product of the form (see Eq.(30))

$$r^*(x_1, x_2, \chi_1, \chi_2) = \psi_q^*(x_1 + 0.5\chi_1, x_2 + 0.5\chi_2) \psi_q(x_1 - 0.5\chi_1, x_2 - 0.5\chi_2)$$

we get the image of Fig.7 (right) with the shift of the cross-terms along the vertical line.

Ambiguity functions of monogenic signals $\psi_M(x_1, x_2)$.



Fig

Fig.8 Left, mesh image, center, surface image of $|AF_M(\mu_1, \mu_2, 0, 0)|$, and right, surface image of

$|AF_M(\mu_1, \mu_2, 0.1, 0.1)|$.

The cross-sections of the magnitude of the ambiguity function of the monogenic version of the test signal (38) are displayed in Figs.8 and should be compared with the cross-sections $|AF_q|$ of Fig.6 and 7. Differently to Fig.6 (center) the function $|AF_M(\mu_1, \mu_2, 0, 0)|$ of Fig.8 (center) shows that the duplicates of the cross-terms are shifted along both the horizontal and vertical lines. For the function $|AF_M(\mu_1, \mu_2, 0.1, 0.1)|$ (nonzero values of the shift variables) the crest values of the cross-terms are enhanced w.r.t. the auto-term and change the support from circular to elliptical shape.

7.2. Images for the AF's and WD's of low-pass signals (see Eq.36).

The cross-sections are presented for fixed values of the spatial coordinates ($\chi_1 = \chi_{10}, \chi_2 = \chi_{20}$) and the following values of the correlation coefficient: $R = 0$ and $R = 0.8$

**The following images apply for the correlation coefficient $R = 0$
The Gaussian test signal is a separable function**

Ambiguity functions and Wigner distributions of analytic signals $\psi_1(x_1, x_2)$ and $\psi_2(x_1, x_2)$

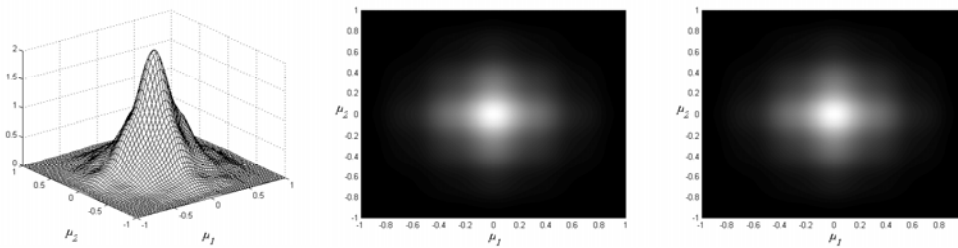


Fig.9. Left, mesh image, center, surface image of $AF_1(\mu_1, \mu_2, 0, 0)$, and right, of $AF_2 = AF_1$.

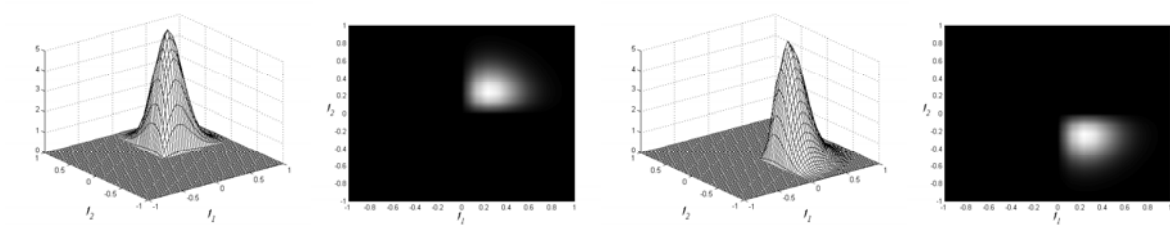


Fig.10. Left: The cross-section of the Wigner distribution $W_1(0,0,f_1,f_2)$ and right of $W_2(0,0,f_1,f_2)$.

For $R = 0$ the Gaussian test signal (40) is a separable function $u(x_1, x_2) = e^{-\pi x_1^2} e^{-\pi x_2^2}$ and the corresponding analytic signals ψ_1 and ψ_2 have equal energies. Fig.9 displays the magnitudes of the corresponding ambiguity functions. We observe that $|AF_1| = |AF_2|$. The corresponding cross-sections of the Wigner distributions are displayed in Fig.10. They have single-quadrant supports in the first and third quadrant respectively. Again W_2 is a mirror image of W_1 similarly, as in Fig.5 The inverse 4-D inverse Fourier transform (see Eq.(26)) yields the AF_1 and AF_2 . They have equal magnitudes and different phase functions. Fig.11 shows, that the equality of magnitudes apply also for cross-sections with non-zero values of the shift variables.

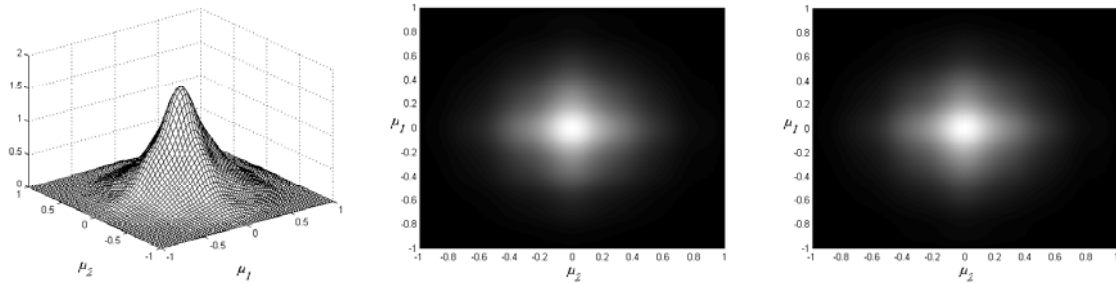


Fig.11. Left: The cross-sections of $|AF_1(\mu_1, \mu_2, 0.5, 0.5)|$, right: of $|AF_2(\mu_1, \mu_2, 0.5, 0.5)|$

Ambiguity functions of the quaternionic signal $\psi_q(x_1, x_2)$

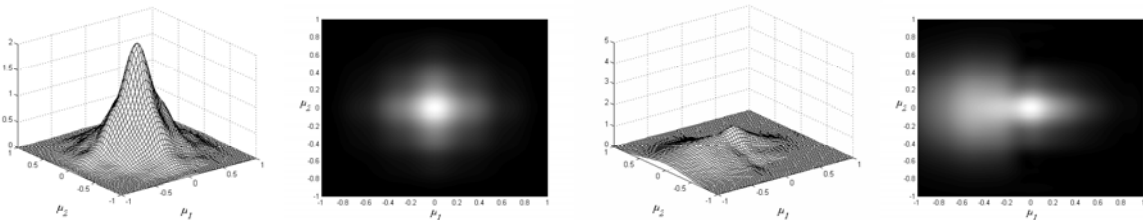


Fig.12. Left: The cross-sections of the magnitude of $|AF_q(\mu_1, \mu_2, 0, 0)|$ and right of $|AF_q(\mu_1, \mu_2, 0.5, 0.5)|$.

The image of Fig.12 (left) shows, that the cross-section $|AF_q(\mu_1, \mu_2, 0, 0)|$ equals the cross-sections $|AF_1(\mu_1, \mu_2, 0, 0)|$ and $|AF_2(\mu_1, \mu_2, 0, 0)|$ of Fig.9. However, the cross-section $|AF_q(\mu_1, \mu_2, 0.5, 0.5)|$ with

non-zero values of the shift variables differ from the cross-sections of Fig.11. Concluding, for non-zero values of the shift variables χ the quaternionic ambiguity function differs considerably from the ambiguity functions of analytic signals.

Ambiguity functions of the monogenic signal $\psi_M(x_1, x_2)$

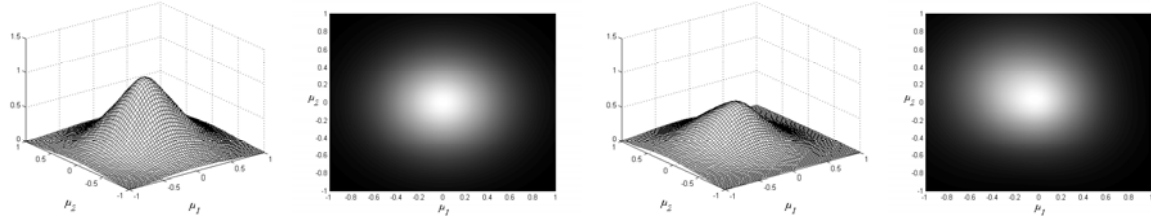


Fig.13. Left: Mesh and surface image of the magnitude of $|AF_M(\mu_1, \mu_2, 0, 0)|$, right: Mesh and surface image of $|AF_M(\mu_1, \mu_2, 0.5, 0.5)|$,

The cross-section of $|AF_M(\mu_1, \mu_2, 0, 0)|$ displayed in Fig.13 (left) is isotropic (circular symmetry), i.e., differs from the corresponding cross-sections of the analytic and quaternionic signals. However, the cross-section $|AF_M(\mu_1, \mu_2, 0.5, 0.5)|$ is unisotropic.

*The following images apply for the correlation coefficient $R = 0.8$
The Gaussian test signal is a nonseparable function*

Ambiguity functions of analytic signals $\psi_1(x_1, x_2)$ and $\psi_2(x_1, x_2)$

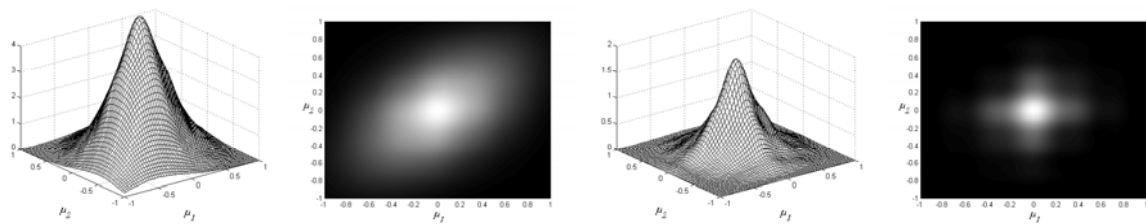


Fig.14 Left, mesh and surface image of $|AF_1(\mu_1, \mu_2, 0, 0)|$ and right the same for $|AF_2(\mu_1, \mu_2, 0, 0)|$

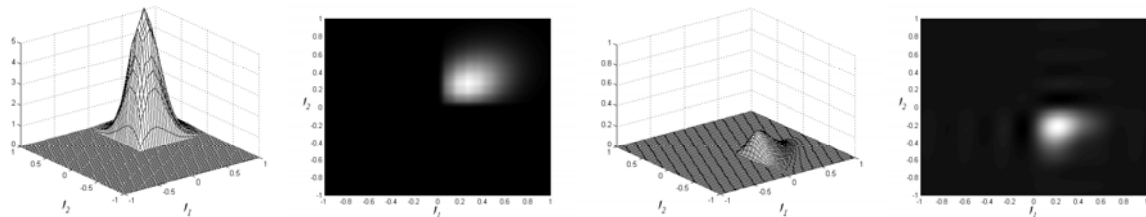


Fig.15. Left, mesh and surface image of $W_1(f_1, f_2, 0, 0)$, and right the same for $W_2(f_1, f_2, 0, 0)$.

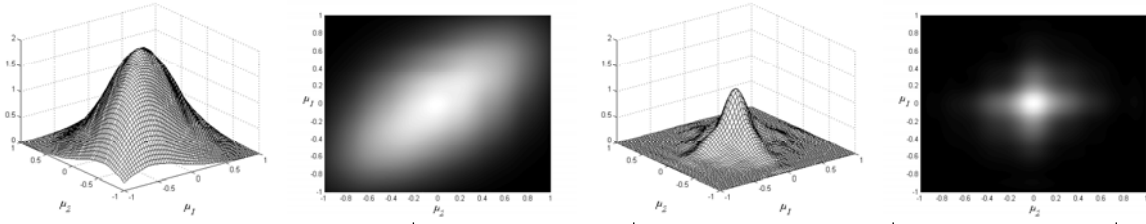


Fig.16 Left, mesh and surface image of $|AF_1(\mu_1, \mu_2, 0.5, 0.5)|$ and right the same for $|AF_2(\mu_1, \mu_2, 0.5, 0.5)|$

For $R = 0.8$ the Gaussian test signal (40) is a non-separable function and the corresponding analytic signals have different energies. In consequence the cross-sections $|AF_1(\mu_1, \mu_2, 0, 0)|$ and

$|AF_2(\mu_1, \mu_2, 0, 0)|$ displayed in Fig.14 have different shapes (compare with Fig.9). The

corresponding cross-sections of the Wigner distributions are displayed in Fig.15. We observe single-quadrant supports in the first and third quadrants respectively. However, W_2 is not the mirror image of W_1 , differently as in Fig.10 for $R = 0$. Notice in Fig.14 the elliptical shape of $|AF_1(\mu_1, \mu_2, 0, 0)|$, In priciple, the cross sections of $|AF_1|$ and $|AF_2|$ with the shift variables equal

$\chi_1 = 0.5, \chi_2 = 0.5$ are the same, as in Fig.14, but with smaller crest values. However, the

corresponding cross-section $|AF_q(\mu_1, \mu_2, 0, 0)|$ of the quaternionic signal displayed in Fig.17

(left) has a symmetric shape . Differently, the cross-section

$|AF_q(\mu_1, \mu_2, 0.5, 0.5)|$ is strongly asymmetric

Ambiguity functions of the quaternionic signal $\psi_q(x_1, x_2)$

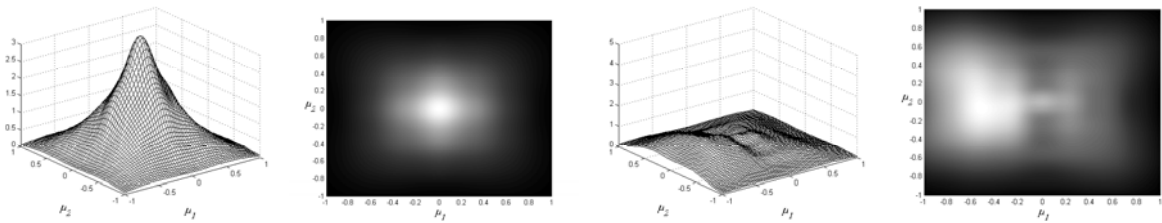


Fig.17. Left: Mesh and surface image of $|AF_q(\mu_1, \mu_2, 0, 0)|$, right: of $|AF_q(\mu_1, \mu_2, 0.5, 0.5)|$,

Ambiguity functions of the monogenic signal $\psi_M(x_1, x_2)$

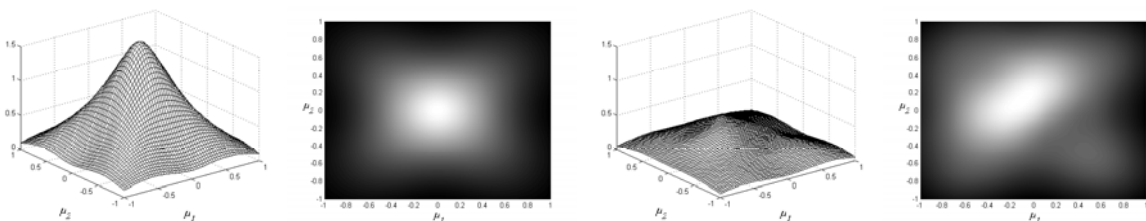


Fig.18. Left: Mesh and surface image of $|AF_M(\mu_1, \mu_2, 0, 0)|$, right: of $|AF_M(\mu_1, \mu_2, 0.5, 0.5)|$

t

The cross-section $|AF_M(\mu_1, \mu_2, 0, 0)|$ of the monogenic signal of Fig.18 has a circular symmetry despite the elliptical shape of the support of the spectrum of the test signal. However, the cross-section $|AF_M(\mu_1, \mu_2, 0.5, 0.5)|$ is asymmetric.

8. Conclusions

A possible method of investigation of bio-medical images is the application of 4-D Wigner distributions or ambiguity functions. Of course, in applications, we have to calculate distributions for real life images. This paper may be classified as an help in choosing the right method of presentation. The use of distributions of analytic, quaternionic or monogenic signals is highly advisable from the point of view of reduction of the number of unwanted cross-terms. This paper investigates the differences between the ambiguity functions of analytic, quaternionic and monogenic signals using simple test signals. We already argued, that the choice of more complicated test signals or eventually real life images makes the comparisons difficult or even impossible. As regards the choice of analytic, quaternionic and monogenic signals, let us recall, that :

1. In general, a given real signal $u(x_1, x_2)$ is represented by two analytic signals $\psi_1(x_1, x_2)$ and $\psi_2(x_1, x_2)$ and in consequence by two ambiguity functions AF_1 and AF_2 of two Wigner distributions W_1 and W_2 .
2. The authors of a notion of a quaternionic signal [6] argued, that a single quaternionic signal $\psi_q(x_1, x_2)$ replaces the two above mentioned analytic signals. In consequence, we get a single quaternionic ambiguity function AF_q and a single Wigner distribution W_q . This integration the two images of $|AF_1|$ and $|AF_2|$ into a single image of $|AF_q|$ works well for separable signals, but only for the cross-sections with zero-values of the shift variables χ (compare Fig.2 (left), with Fig.6 (left)). For non-zero values of the shift variables the above mentioned integration of two images to a single one produces a lot of shifted cross-terms (see Fig. 6 and Fig. 7) and in the case of a low pass

signal a highly distorted and an-isotropic image (see Fig. 12) . These effects should be examined by the choice of the ambiguity functions

3. Similar remarks apply for the eventual choice of ambiguity functions of monogenic signals. The authors of the notion of a monogenic signal [7] used the isotropic Riesz transforms instead of the nonisotropic Hilbert transforms. However, the ambiguity functions of monogenic signals produce shifted cross-terms along in both the horizontal as vertical lines also for zero values of the shift variables (see Fig.8). For non-zero values of these variables all the cross-terms are enhanced w.r.t. the auto-term. For the non-separable low-pass Gaussian signal ($R = 0.8$) the image of $|AF_M|$ is isotropic only for zero valued shift variables and highly an-isotropic otherwise (se Fig.18). In consequence the advantages of application of ambiguity functions of monogenic signals are questionable.

Let us mention again that only Wigner distributions of analytic signals are real functions and the Wigner distributions of quaternionic and monogenic signals may be quaternionic valued..Differently, the ambiguity functions AF_1 and AF_2 may be complex and AF_q or AF_M may be quaternionic valued.. For all ambiguity functions we presented the cross-sections of the magnitudes omitting the presentation of phase functions. The ambiguity functions AF_1 and AF_2 are represented each by a single 2-D phase function defined by the polar form of the Eq.(25). Differently, the quaternionic ambiguity function AF_q is represented by three phase functions, or two for separable signals. The monogenic ambiguity function AF_M is represented by two phase functions.

It seems that comparisons of the features of ambiguity functions using phase functions would be a difficult task.

Acknowledgement

This research is supported by the grant Nr.4 T!!D01222 of KBN (Committee of Scientific Research of the Polish Ministry of Science).

References

1. Woodward P.M., : Information theory and design of radar receivers. Proceedings of the Institute of Radio Engineers, 1951, **40**, pp.1521-1524.
2. Wigner E.P.,: On the quantum correction for thermodynamic equilibrium. Phys. Rev., vol. 40, pp. 749-752, 1932.
3. Hahn S.L., : Multidimensional complex signals with single-orthant spectra. Proc. IEEE, vol. 80,

- No. 8, Aug.1992, pp. 1287-1300.
4. Hahn S.L., : Hilbert Transforms in Signal Processing. Artech House, 1996.
 5. Bülow T., : Hypercomplex spectral signal representation for the processing and analysis of images. Bericht Nr. 9903, Institut für Informatik und Praktische Mathematik, Christian-Albrechts-Universität Kiel, Aug. 1999.
 - 6 Bülow T., Sommer G., : The Hypercomplex Signal - A Novel Extension of the Analytic Signal to the Multidimensional Case. IEEE Trans. Signal Processing, vol. 49, No. 11, pp. 2844-2852, Nov. 2001.
 7. Felsberg M., : Low-Level Image Processing with the Structure Multivector. Institute of Computer Science and Applied Mathematics, Christian-Albrechts-University of Kiel, Report No. 0203, 2002.
 8. Felsberg M., Sommer G., : The Monogenic Signal. IEEE Trans. Signal Processing, vol.49, No. 12, pp. 3136-3140, Dec. 2001.
 9. Sommer G. (Ed.) :Geometric Computing with Clifford Algebra. Theoretical Foundations and Applications in Computer Vision and Robotics. ISBN 3-540-41198-4, Springer Verlag Berlin Heidelberg 2001.
 10. Larkin K.G., Bone D., Oldfield M.A., : Natural demodulation of two-dimensional fringe patterns: I. General background of the spiral phase quadrature transform. J. Opt. Soc. Am., vol.18, No.8, pp.1862-1870, Aug. 2001.
 11. Hahn S.L., : A review of methods of time-frequency analysis with extension for signal plane-frequency plane analysis. Kleinheubacher Berichte, Band 44, pp. 163-182, 2001.
 12. Hahn S.L., : The theory of time-frequency distributions with extension for two-dimensional signals. Metrology and Measurements Systems, Vol. VIII, No. 2, pp. 113-143, 2000.
 13. Hahn S.L., Snopek K.M., : Wigner Distributions and Ambiguity Functions in Image Analysis. Computer Analysis of Images and Patterns edited by W. Skarbek, Springer Verlag, pp. 537-546, 2001.
 14. Hahn S.L., Snopek K.M., : Wigner distributions and ambiguity functions of 2-D Quaternionic and monogenic signals., in print in IEEE Trans. on Signal Processing (2005)..

Appendix A: The derivations of ambiguity functions.

Notations: For any function the superscript „+” indicates $f^+ = f(x_1 + \chi_1/2, x_2 + \chi_2/2)$ and „-”, indicates $f^- = f(x_1 - \chi_1/2, x_2 - \chi_2/2)$.

A1. Ambiguity functions of the analytic signals

Let us write the Eqs.(3) and (4) in the common form

$$\psi_{1,2}(x_1, x_2) = u \mp v + j(v_1 \pm v_2) = \text{Re}_{1,2} + j \text{Im}_{1,2} \quad (\text{A.1})$$

with upper signs applying for ψ_1 and lower signs for ψ_2 . The ambiguity functions of ψ_1 and ψ_2 are:

$$\begin{aligned}
AF_{1,2}(\mu_1, \mu_2, \chi_1, \chi_2) &= \iint \psi_{1,2}^+ \psi_{1,2}^- e^{j2\pi(\mu_1 x_1 + \mu_2 x_2)} dx_1 dx_2 = \\
&\iint (\text{Re}_{1,2}^+ + j\text{Im}_{1,2}^+) (\text{Re}_{1,2}^- - j\text{Im}_{1,2}^-) \left\{ \cos \left[2\pi(\mu_1 x_1 + \mu_2 x_2) \right] + j \sin \left[(\mu_1 x_1 + \mu_2 x_2) \right] \right\} dx_1 dx_2 \\
&= \iint \left[\text{Re}_{1,2}^+ \text{Re}_{1,2}^- + \text{Im}_{1,2}^+ \text{Im}_{1,2}^- \right] \cos \left[2\pi(\mu_1 x_1 + \mu_2 x_2) \right] dx_1 dx_2 \\
&\quad + j \iint \left[\text{Im}_{1,2}^+ \text{Re}_{1,2}^- - \text{Im}_{1,2}^- \text{Re}_{1,2}^+ \right] \sin \left[2\pi(\mu_1 x_1 + \mu_2 x_2) \right] dx_1 dx_2 \\
&= \text{Re} \left[AF_{1,2} \right] + j \text{Im} \left[AF_{1,2} \right] \tag{A.2}
\end{aligned}$$

The polar form $AF_{1,2} = |AF_{1,2}| \exp[j\Phi]$ defines the magnitude and the phase function.

A.2. Ambiguity function of the quaternionic signal

The quaternionic signal defined by the Eq.(11) is

$$\psi_q(x_1, x_2) = u + iv_1 + jv_2 + kv^3$$

The ambiguity function is defined by the inverse *QFT*

$$AF_q(\mu_1, \mu_2, \chi_1, \chi_2) = \iint e^{i2\pi\mu_1 x_1} \psi_q^+ \psi_q^{-*} e^{j2\pi\mu_2 x_2} dx_1 dx_2 \tag{A.3}$$

Let us use the notation $\alpha_1 = 2\pi\mu_1 x_1$, $\alpha_2 = 2\pi\mu_2 x_2$. We can continue:

$$\iint \left[\cos(\alpha_1) + i \sin(\alpha_1) \right] \left[A + iB + jC + kD \right] \left[\cos(\alpha_2) + j \sin(\alpha_2) \right] dx_1 dx_2, \tag{A.4}$$

where

$$A = u^+ u^- + v_1^+ v_1^- + v_2^+ v_2^- + v^+ v^- ; \quad B = v_1^+ u^- - u^+ v_1^- + v^+ v_2^- - v_2^+ v^- ; \tag{A.5}$$

$$C = v_2^+ u^- - v^+ v_1^- - u^+ v_2^- + v_1^+ v^- ; \quad D = v^+ u^- + v_2^+ v_1^- - v_1^+ v_2^- - u^+ v^- . \tag{A.6}$$

Performing the multiplications and using the algebra of quaternions yields the following quaternion valued ambiguity function :

$$\begin{aligned}
&AF_q(\mu_1, \mu_2, \chi_1, \chi_2) \tag{A7} \\
&= \iint \left[\cos(\alpha_1) \cos(\alpha_2) A - \sin(\alpha_1) \cos(\alpha_2) B - \cos(\alpha_1) \sin(\alpha_2) C + \sin(\alpha_1) \sin(\alpha_2) D \right] dx_1 dx_2
\end{aligned}$$

$$\begin{aligned}
& +i\iint\left[\cos(\alpha_1)\cos(\alpha_2)B+\sin(\alpha_1)\cos(\alpha_2)A-\cos(\alpha_1)\sin(\alpha_2)D-\sin(\alpha_1)\sin(\alpha_2)C\right]dx_1dx_2 \\
& +j\iint\left[\cos(\alpha_1)\cos(\alpha_2)C-\sin(\alpha_1)\cos(\alpha_2)D+\cos(\alpha_1)\sin(\alpha_2)A-\sin(\alpha_1)\sin(\alpha_2)B\right]dx_1dx_2 \\
& +k\iint\left[\cos(\alpha_1)\cos(\alpha_2)D+\sin(\alpha_1)\cos(\alpha_2)C+\cos(\alpha_1)\sin(\alpha_2)B+\sin(\alpha_1)\sin(\alpha_2)A\right]dx_1dx_2.
\end{aligned}$$

Let us write the above AF_q in the form

$$AF_q(\mu_1, \mu_2, \chi_1, \chi_2) = A_q + iB_q + jC_q + kD_q \quad (\text{A8})$$

where A_q , B_q , C_q and D_q are given by the above integrals. The magnitude of AF_q is

$$|AF_q| = \sqrt{A_q^2 + B_q^2 + C_q^2 + D_q^2} \quad (\text{A9})$$

and the polar form $AF_q = |AF_q| e^{i\phi_q + j\phi_{qj} + k\phi_{qk}}$ defines three phase functions.

A3. Ambiguity function of the monogenic signal

The monogenic signal is defined by the Eq.(13):

$$\psi_M(x_1, x_2) = u + iv_{r1} + jv_{r2}.$$

The correlation product is:

$$r_M(x_1, x_2, \chi_1, \chi_2) = \psi_M^+ \psi_M^{*-} = [u^+ + iv_{r1}^+ + jv_{r2}^+] [u^+ - iv_{r1}^- - jv_{r2}^-] \quad (\text{A.10})$$

The derivation is the same, as for quaternionic signals with:

$$A_M = u^+ u^- + v_{r1}^+ v_{r1}^- + v_{r2}^+ v_{r2}^- \quad ; \quad B_M = v_{r1}^+ u^- - u^+ v_{r1}^- \quad ; \quad (\text{A11})$$

$$C_M = v_{r2}^+ u^- - u^+ v_{r2}^- \quad ; \quad D_M = v_{r2}^+ v_{r1}^- - v_{r1}^+ v_{r2}^- \quad . \quad (\text{A.12})$$

and

$$AF_M(\mu_1, \mu_2, \chi_1, \chi_2) = A_M + iB_M + jC_M + kD_M \quad (\text{A13})$$

$$|AF_M| = \sqrt{A_M^2 + B_M^2 + C_M^2 + D_M^2} \quad (\text{A14})$$

and analogously to the quaternionic case the polar form $AF_M = |AF_M| e^{i\phi_{M_i} + j\phi_{M_j} + k\phi_{M_k}}$ defines

three phase functions. Let us mention, that the representation of the monogenic signal in

spherical coordinates (r, θ, ϕ) defines two phase functions.

A 4. The calculation of ambiguity functions using frequency domain algorithms.

1. Analytic signals.

Consider a real signal $u(x_1, x_2)$ and its Fourier transform $U(f_1, f_2)$. The single quadrant spectra of ψ_1 and ψ_2 are:

$$\Gamma(f_1, f_2) = [1 + \text{sgn}(f_1)] [1 \pm \text{sgn}(f_1)] U(f_1, f_2) = \text{Re}_{1,2} + j \text{Im}_{1,2} \quad (\text{A15})$$

where the „+” sign stands for Γ_1 and „-” sign for Γ_2 . The ambiguity functions are:

$$AF_{1,2}(\mu_1, \mu_2, \chi_1, \chi_2) = \iint \Gamma_{1,2}^+ \Gamma_{1,2}^{-*} e^{j2\pi(f_1\chi_1 + f_2\chi_2)} df_1 df_2 \quad (\text{A16})$$

Let us denote $s_1 = [1 + \text{sgn}(f_1)]$ and $s_2 = [1 + \text{sgn}(f_2)]$. We get

$$AF_{1,2}(\mu_1, \mu_2, \chi_1, \chi_2) = \iint s_1^+ s_2^+ s_1^- s_2^- U^+ U^{-*} e^{j2\pi(f_1\chi_1 + f_2\chi_2)} df_1 df_2 \quad (\text{A17}).$$

Using the notation:

$$s_1^+ s_2^+ s_1^- s_2^- U^+ U^{-*} = \text{Re} + j \text{Im}$$

we get

$$\begin{aligned} AF_{1,2}(\mu_1, \mu_2, \chi_1, \chi_2) = & \iint \left[\left[\text{Re} \cos[2\pi(f_1\chi_1 + f_2\chi_2)] + \text{Im} \sin[2\pi(f_1\chi_1 + f_2\chi_2)] \right] \right] df_1 df_2 \\ & + j \iint \left[\left[\text{Im} \cos[2\pi(f_1\chi_1 + f_2\chi_2)] - \text{Re} \sin[2\pi(f_1\chi_1 + f_2\chi_2)] \right] \right] df_1 df_2. \end{aligned}$$

We get

$$AF_{1,2}(\mu_1, \mu_2, \chi_1, \chi_2) = \text{Re}[AF_{1,2}] + j \text{Im}[AF_{1,2}].$$

There is a strict evidence, that for analytic signals the spatial domain and frequency domain algorithms define exactly the same ambiguity functions.

2. Quaternionic and monogenic signals.

No evidence exists for the equality of ambiguity functions calculated in the spatial domain and frequency domain. For the test signals used in this paper, the frequency domain algorithm yields $AF_q = AF_1$, since ψ_1 and ψ_q have equal single-quadrant spectra. As well, the frequency domain algorithm of calculation the monogenic ambiguity function

yields a different distribution, as the spatial domain algorithm. In consequence, for quaternionic and monogenic signals the frequency domain algorithms yield another functions in respect to the spatial domain algorithms .